

ORIGINAL ARTICLE

Perylene bisimide organogels formed by melamine · cyanurate/barbiturate hydrogen-bonded tapes

Tomohiro Seki, Takashi Karatsu, Akihide Kitamura and Shiki Yagai

Ditopic melamines possessing one (1) or two (2) perylene bisimide (PBI) chromophores were synthesized and their self-aggregation and coaggregation with dodecyl cyanurate (dCA) or barbital (Bar) were investigated. Optically transparent organogels were formed through self-aggregation of 1 and coaggregation of 1 or 2 with dCA or Bar in nonpolar solvents. X-ray diffraction of the xerogels exhibited typical diffraction patterns assignable to lamellar structures, suggesting the formation of tapelike hydrogen-bonded motifs. Remarkably low critical gelation concentrations (*cgc*) of 8.0×10^{-4} M were revealed for all organogels, thus they can be classified as supergelators. Comparison of the thermal stabilities of the gels revealed that the gels containing 2 have higher melting temperatures (T_m) than those containing 1. Scanning electron microscopy and atomic force microscopy showed that the gels containing 1 are composed of sheetlike microstructures, whereas those containing 2 are composed of fibrous nanostructures, consistent with the difference in their thermal stabilities. The different self-assembled structures of our PBI aggregates can be related to whether extended stacks of PBI dyes along the hydrogen-bonded strands are possible or not. *Polymer Journal* (2012) 44, 600–606; doi:10.1038/pj.2012.22; published online 21 March 2012

Keywords: hydrogen bond; organogel; perylene bisimide; self-assembly; supramolecular chemistry

INTRODUCTION

Supramolecular assemblies of functional π -systems are an intriguing topic of chemical researches because self-assembled architectures could be controlled in nano- to micrometer scales by supramolecular designs based on a variety of noncovalent interactions.^{1–3} Among various functional π -systems, perylene bisimide (PBI) dyes have received considerable attention owing to their high chemical and thermal stabilities, *n*-type semiconductivity and outstanding optical properties.^{4,5} Therefore, it is not surprising that diverse functional soft-materials composed of self-assembled PBI dyes have been reported.^{6–17} For example, organogels^{18,19} of PBI dyes have been constructed through various noncovalent interactions,^{11–17} and their utility have already been demonstrated by a variety of applications, such as light harvesting systems,¹⁴ photovoltaic devices¹⁵ and electron transporting materials.^{16,17}

As a reliable tool to control the self-assembly of functional dye molecules, we have effectively employed complementary multiple hydrogen bonding interactions between melamine and cyanurate or barbiturate.^{20,21} Proper molecular design leads to the formation of well-defined hydrogen-bonded species, such as cyclic hexamers so called rosettes,²² 3 + 1 discotics,^{17,23} 1 + 1²⁴ or 2 + 2 closed species,²⁵ rigid²⁶ or flexible supramolecular polymers^{6,11,12,27} and so on, as the lowest level of their organization. Such hydrogen-bonded species can hierarchically organize into higher order aggregates through π – π

stacking interactions of dye components. A well-defined relationship between hydrogen-bonded species and hierarchically organized structures enables us to prepare predictable mesoscopic superstructures involving functional dyes.²⁸ For PBI dyes, we have recently succeeded to organize soluble swallow-tailed derivatives, which inherently form one-dimensional columnar structures,^{29,30} into two-dimensional lamellar structures²⁶ by using linear tapelike hydrogen bonding motifs of melamine-cyanurate (2 · dCA) or melamine-barbiturate (2 · Bar, Figures 1 and 2).^{31–34} These aggregates are highly soluble in halogenated solvents such as chloroform, thus enabling the fabrication of smooth thin films without notable grain boundaries via solution processing followed by thermal annealing. The resulting thin films could be used as electron transporting layers in organic field effect transistor (OFET) devices.²⁶

In the present study, we focused on the gelation properties of these hydrogen-bonded tapes of PBI in less polar organic solvents. Because hydrogen-bond-directed aggregation of 2 alone and 2 · Bar/dCA is considered to be stabilized cooperatively by extended π – π stacking of PBI dyes, we also prepared monochromophoric derivative 1 to investigate such an effect. As a result, the gelation properties of 1 and 2 were found to depend differently on the complementary guest molecules and the solvent polarity. Furthermore, distinct mesoscopic structures, i.e., two-dimensional sheets and one-dimensional fibers, were formed for xerogels of 1 and 2, respectively, suggesting that

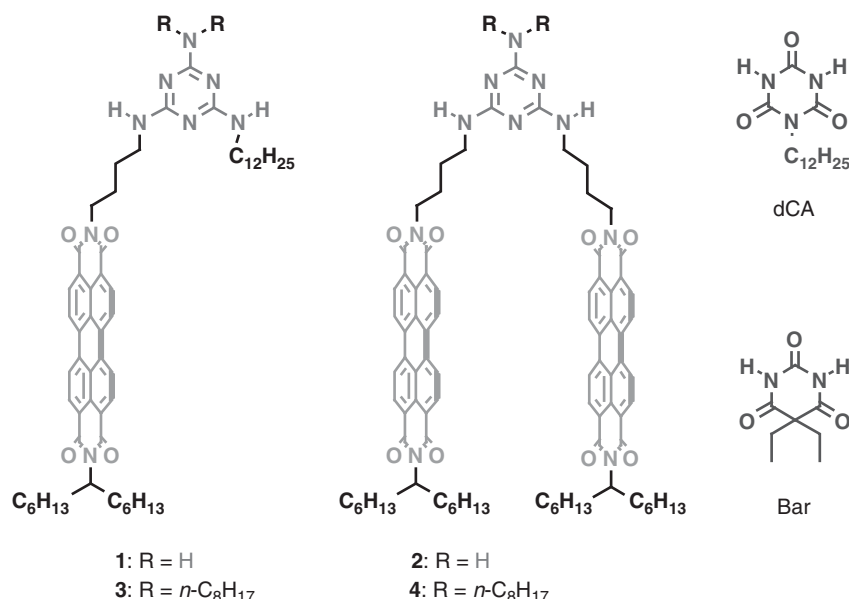


Figure 1 Structures of PBI-functionalized melamines **1–4**, and dodecyl cyanurate (dCA) and barbital (Bar). A full color version of this figure is available at *Polymer Journal* online.

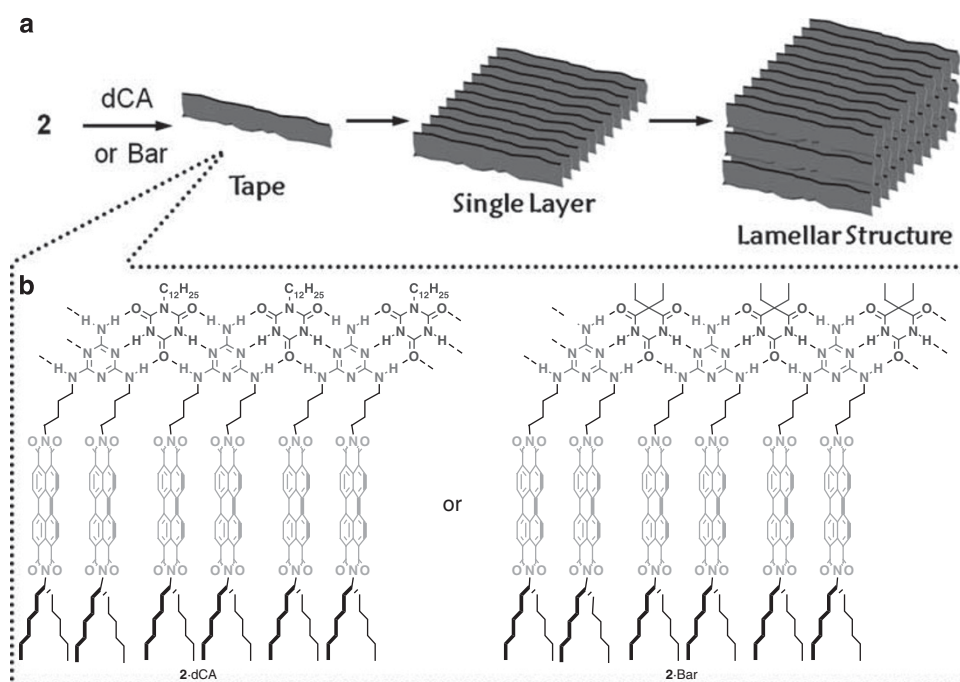


Figure 2 (a) Schematic representation of hierarchical organization of hydrogen-bonded tapes of **2**·dCA and **2**·Bar. (b) Proposed structures of hydrogen-bonded tapes. A full color version of this figure is available at *Polymer Journal* online.

the π - π stacking interaction between PBI moieties control the dimensionality of the hierarchical organization of the hydrogen-bonded tapes.

RESULTS AND DISCUSSION

UV/vis studies

The synthesis of ditopic melamine **2** possessing two PBI chromophores was reported previously.²⁶ In this study, we newly prepared a monochromophoric compound **1** by introducing dodecyl chain instead of one of the two perylene pendants in **2** (see Supple-

mentary Information). We also prepared compounds **3** and **4** as references lacking ditopic binding capability (Figure 1).

UV/vis titration of **1** with dCA was performed in methylcyclohexane (MCH) at a concentration of 1.4×10^{-5} M. In the absence of dCA, **1** exhibited a spectrum characteristic of π - π stacked perylene chromophores (red line in Figure 3). The spectrum is in sharp contrast to a vibronically structured one typical of the molecularly-dissolved PBI chromophores observed for the reference compound **3** under the same condition (blue line in Figure 3). This result indicates that hydrogen bonding between ditopic melamine moieties promotes

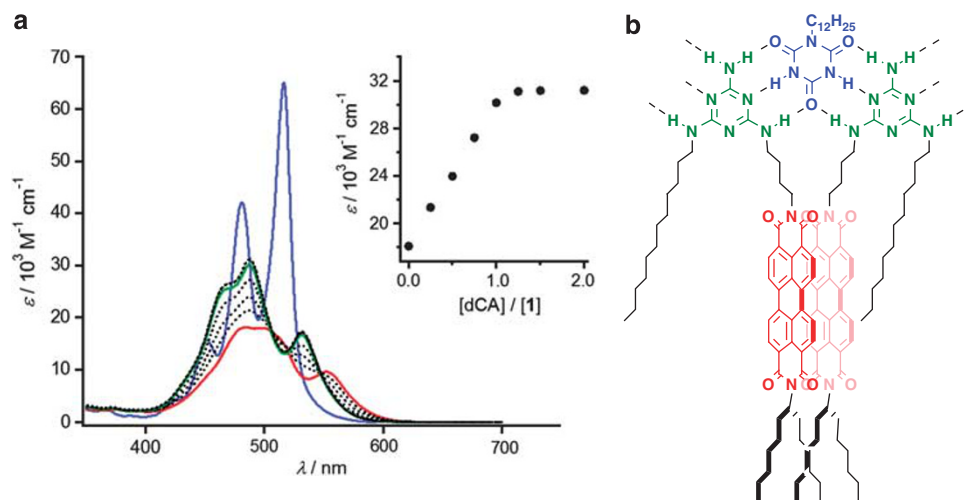


Figure 3 (a) UV/vis spectra of MCH solutions containing constant amount of **1** ($c = 1.4 \times 10^{-5} \text{ M}$) and various amounts of dCA ($c = 0$ to $2.8 \times 10^{-5} \text{ M}$) at 25°C . The spectra of pure **1** and of 1:1 mixture with dCA are colored with red and green, respectively. The blue curve shows the spectrum of reference compound **3** ($c = 1.4 \times 10^{-5} \text{ M}$) in MCH. Inset shows plot of ϵ at 487 nm versus $[\text{dCA}]/[\mathbf{1}]$. (b) Local binding motif of **1** · dCA showing PBI moieties of **1** form an intermolecular dimeric stack locked by a melamine-cyanurate-melamine interaction.

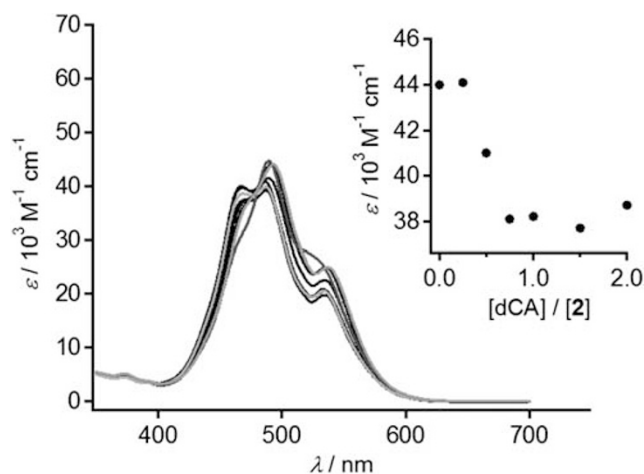


Figure 4 UV/vis spectra of MCH solutions containing constant amount of **2** ($c = 1.4 \times 10^{-5} \text{ M}$) and various amounts of dCA ($c = 0$ to $2.8 \times 10^{-5} \text{ M}$) at 25°C . The spectra of pure **2** and of their 1:1 mixture with dCA are colored with red and green, respectively. The blue curve shows the spectrum of reference compound **4** ($c = 1.4 \times 10^{-5} \text{ M}$) in MCH. Inset shows plot of ϵ at 492 nm versus $[\text{dCA}]/[\mathbf{2}]$. A full color version of this figure is available at *Polymer Journal* online.

the π - π stacking aggregation of **1**. Upon addition of dCA, the spectrum of **1** underwent hyperchromic change with a hypsochromic shift (green line in Figure 3). This spectral transition indicates that the stacking arrangement of PBI chromophores changes upon binding with dCA. More vibronically structured spectra in the presence of dCA may reflect the formation of dimeric perylene stacks with restricted rotational displacement by the melamine-cyanurate-melamine array (Figure 3b).^{17,23,25,35} The plot of the absorption intensity at 487 nm versus $[\text{dCA}]/[\mathbf{1}]$ exhibited a kink at a molar ratio of 1:1 (inset in Figure 3a), indicating the 1:1 aggregation.

The UV/vis titration experiment with dCA was also performed for bichromophoric derivative **2** in MCH. However, the spectra of **2** showed only a minor change upon increasing concentration of dCA (red to green spectra in Figure 4). This result can be reasonably

Table 1 Gelation properties of **1** and **2** and their coaggregates with dCA or Bar

	Chloroform	Toluene	MCH
1	S	S	G / $T_m^a = 45^\circ \text{C}$ ($c_{gc}^b = 8.0 \times 10^{-4} \text{ M}$)
1 · dCA	S	S	G / $T_m^a = 65^\circ \text{C}$ ($c_{gc}^b = 8.0 \times 10^{-4} \text{ M}$)
1 · Bar	S	S	P
2	P	I	I
2 · dCA	S	S	I
2 · Bar	S	G / $T_m^a = 110^\circ \text{C}$ ($c_{gc}^b = 8.0 \times 10^{-4} \text{ M}$)	I

Concentrations of gelators: $5.0 \times 10^{-3} \text{ M}$. **S**: homogeneous solution, **I**: insoluble, **P**: precipitates, **G**: transparent gel.

^aMelting temperatures (T_m) were measured by using gels at concentration of $5.0 \times 10^{-3} \text{ M}$.

^bCritical gelation concentrations.

explained by the intramolecular π - π stacking of PBI chromophores in **2**, which was further supported by reference compound **4** exhibiting a spectrum similar to those of **2** (blue line in Figure 4). Because of such minor spectral change upon aggregation with dCA, the plot of ϵ at certain wavelength versus $[\text{dCA}]/[\mathbf{2}]$ does not clearly confirm 1:1 aggregation (inset in Figure 4). Instead, the use of toluene, a more polar solvent than MCH, gave a more reasonable binding isotherm to conclude 1:1 aggregation (Supplementary Figure S1).²⁶

Gelation studies

Gelation experiments were performed for pure PBIs **1** and **2**, and their coaggregated mixtures with dCA or Bar (i.e., **1** · dCA, **1** · Bar, **2** · dCA and **2** · Bar) and the results were summarized in Table 1. Chloroform, toluene and MCH were chosen as solvents and concentrations of the compounds were set to $5.0 \times 10^{-3} \text{ M}$. For gelation test, solvent was directly added to solid samples and refluxed until all the solids were dissolved. The resulting homogeneous solutions were then cooled to room temperature. After the solutions were kept at room temperature

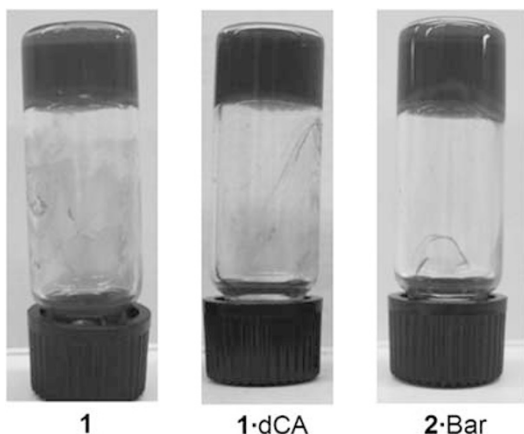


Figure 5 Photographs of MCH organogels of **1** and **1·dCA** and toluene organogel of **2·Bar**. Concentrations of gelators: 5.0×10^{-3} M. A full color version of this figure is available at *Polymer Journal* online.

for 1 h, gelation was checked by the 'stable-to-inversion of a vial' method.³⁶

PBI **1** formed homogeneous solutions in all the above solvents upon heating, but only MCH solutions turned into transparent organogels upon cooling (Figure 5). Transparent organogels are promising materials for application in optoelectronic devices, because unfavorable scattering of visible light may not occur. In contrast, PBI **2** could be dissolved only in chloroform upon heating, but precipitation took place upon cooling.

The solid samples of mixtures **1·dCA**, **1·Bar**, **2·dCA** and **2·Bar** could not be dissolved in any of these three solvents with prolonged refluxing. These failures might be due to the low solubilities of either or both of the individual components. In order to assess the gelation capabilities of these systems as 'hydrogen-bonded coaggregates', we thus dissolved the solid mixtures in 20 v/v% chloroform/methanol mixture, where all of the individual components are soluble. Upon evaporating the solvents, homogeneously red-colored solids were obtained for all the systems, and they could be dissolved in pure

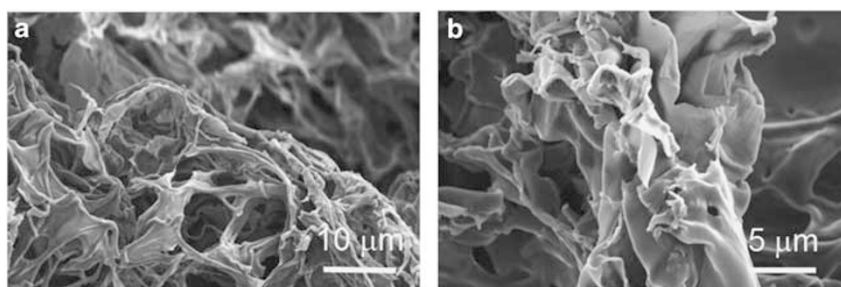


Figure 6 SEM images of dried MCH gels ($c = 5.0 \times 10^{-3}$ M) of (a) **1** and (b) **1·dCA**.

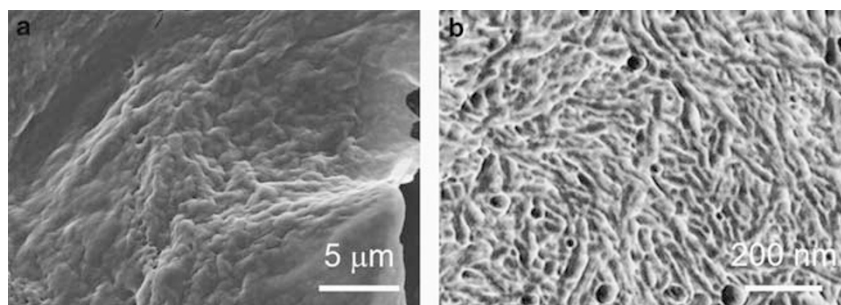


Figure 7 (a) SEM image of dried toluene gel ($c = 5.0 \times 10^{-3}$ M) of **2·Bar**. (b) AFM image of dried toluene gel ($c = 1.0 \times 10^{-3}$ M) of **2·Bar**. A full color version of this figure is available at *Polymer Journal* online.

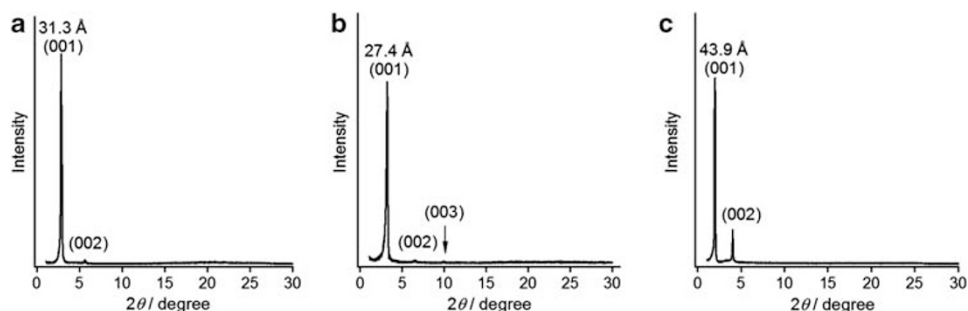


Figure 8 XRD patterns of dried gels of (a) **1**, (b) **1·dCA** and (c) **2·Bar** at room temperature. The thin films were annealed at 130 °C for **1**, 230 °C for **1·dCA** and 240 °C for **2·Bar** for 5 min prior to measurements.

chloroform without thermal treatment to give homogeneous solutions. The observed increase of the solubility of complementary components upon mixing have been commonly observed, and this is a clear indication of the formation of coaggregates through triple hydrogen bonds.^{20,21,31–34,37–39} However, no gelation was observed for all the coaggregate systems in chloroform, indicating that the resulting hydrogen-bonded species exist as oligomeric state in this hydrogen-bond-competing solvent.^{40,41}

When the above four coaggregated mixtures were subjected to gelation experiments using toluene, we could see a clear difference in their aggregation ability because all the aggregates can be readily soluble upon heating. The coaggregated mixtures of **2**·Bar immediately formed an organogel upon cooling to room temperature (Figure 5), whereas **1**·dCA, **1**·Bar and **2**·dCA showed neither gelation nor increase in viscosity. The different gelation ability of **1**·Bar and **2**·Bar clearly demonstrates a crucial role of intramolecular π - π interactions between PBI chromophores. The critical gelation

concentration (c_{gc}) of **2**·Bar is determined to be 8.0×10^{-4} M in toluene (Table 1). Thus, **2**·Bar can be classified as a supergelator,⁴² and only limited examples of PBI supergelators have been reported so far.^{12,14,16} Moreover, we found that **2**·Bar showed a remarkably high thermal stability. When a glass vial ($\phi = 15$ mm) containing a toluene organogel of **2**·Bar ($c = 5.0 \times 10^{-3}$ M) were lying on a hot plate and then heated, the solvent started to flow at 110 °C after 5 min (Table 1). This temperature, referred to as melting temperature (T_m), is close to the boiling point of toluene. Only few examples of functional dye-based organogels with T_m values exceeding 100 °C have been reported.⁴³

For the least polar solvent MCH, coaggregated mixtures **2**·dCA and **2**·Bar were insoluble so that we could not compare their gelation ability. In contrast, **1**·dCA and **1**·Bar were readily soluble in MCH upon heating and only **1**·dCA afforded a transparent organogel upon cooling to room temperature (Figure 5).

Because MCH was successfully gelled by **1** alone and **1**·dCA, we compared the thermal stabilities of these organogels. Both of the coaggregates showed c_{gc} values of 8.0×10^{-4} M (Table 1), which are in the range of supergelator.⁴² Despite the same c_{gc} values, these two organogels showed different T_m values, 45 °C for **1** and 65 °C for **1**·dCA at the concentration of 5.0×10^{-3} M (Table 1). This is a clear indication of the involvement of stronger triple hydrogen bonding interactions in the latter.^{11,12,17,25,35} Temperature-dependant UV/vis absorption studies in MCH under diluted condition indicate that thermal stability of local π -stack interactions of PBI moieties of **1**·dCA is more stable than those of **1**, which is consistent with thermal stabilities of these aggregates in the gel states (Supplementary Figure S2).

Table 2 Results of XRD measurements of six aggregates

	Diffraction (001)	Diffraction (002)	Diffraction (003)
1	31.3 Å	15.6 Å	—
1 ·dCA	27.4 Å	13.6 Å	8.94 Å
1 ·Bar	23.4 Å	11.4 Å	7.83 Å
2	42.2 Å	20.9 Å	—
2 ·dCA	31.1 Å	15.5 Å	—
2 ·Bar	43.9 Å	21.6 Å	—

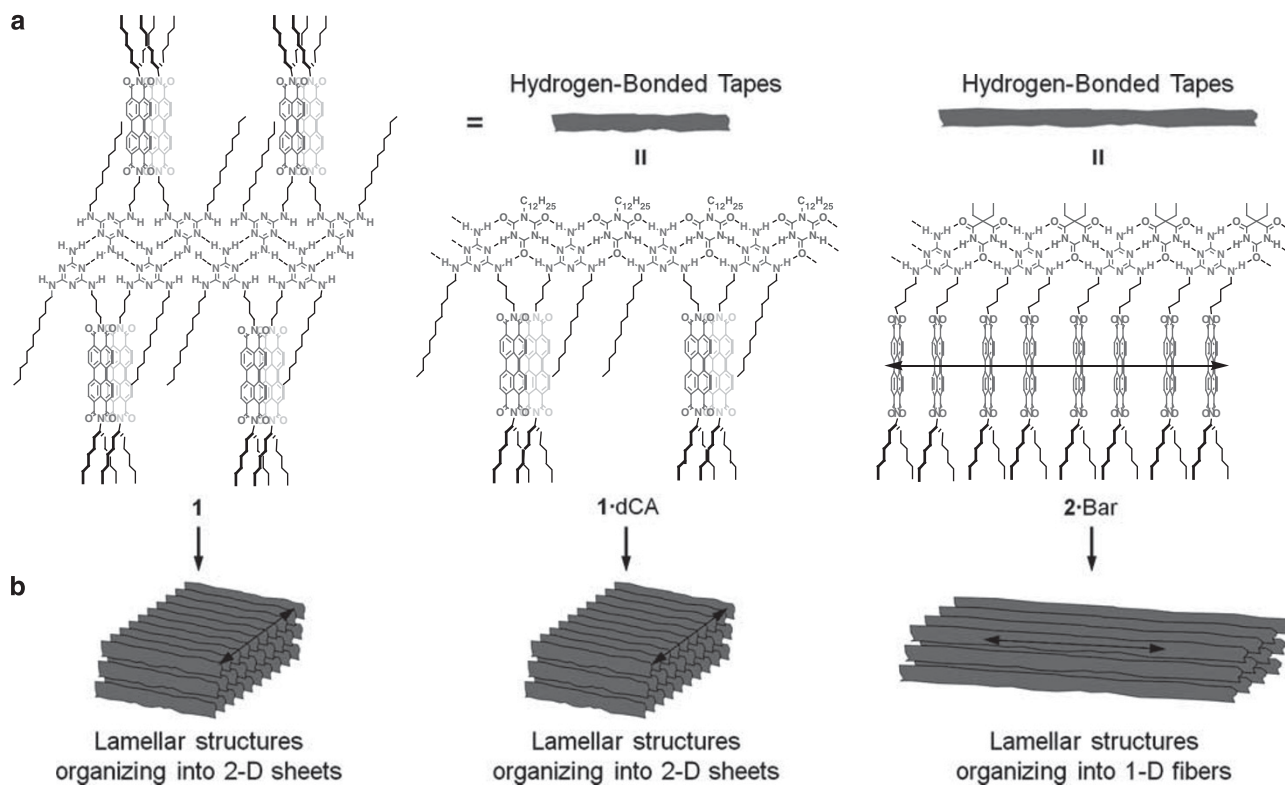


Figure 9 (a) Proposed supramolecular structures of hydrogen-bonded tapes formed by **1**, **1**·dCA and **2**·Bar. (b) Schematic representations of lamellar structures formed by hydrogen-bonded tapes, which organized into sheetlike (**1** and **1**·dCA) or fibrous (**2**·Bar) mesoscopic morphologies. Double arrows indicate favorable growth direction of PBI π -stacks. A full color version of this figure is available at *Polymer Journal* online.

Microscopic structures

Organogels of **1** (MCH), **1**·dCA (MCH) and **2**·Bar (toluene) were freeze-dried, and the resulting xerogels were investigated by scanning electron microscopy (SEM). The SEM images of **1** and **1**·dCA showed sheetlike microscopic structures with smooth surface (Figure 6). The similar sheetlike morphologies have been reported for organogels composed of two-dimensionally organized supramolecular aggregates.^{44,45} In contrast, the SEM image of **2**·Bar displayed self-assembled structures with a grainy surface (Figure 7a). To confirm the presence of finer structures in nanoscopic scale, the surface of the xerogel of **2**·Bar was analyzed by atomic force microscopy (AFM).¹² As shown in Figure 7b, AFM showed entangled networks of fibrous aggregates with widths of around 20 nm, implying the tendency of this system organizing into one-dimensional structures. Such fibrous structures were not observed for **1** and **1**·dCA. It has been reported that organogels with fibrous nanostructures show superior gelation properties (higher T_m and lower c_{gc}) than those with sheetlike ones.⁴⁶ This holds true for our gelator systems because T_m values of **2**·Bar is significantly higher than those of **1** and **1**·dCA even though more polar toluene was employed.

Solvent-free films were prepared from the above organogels and studied by X-ray diffraction (XRD). All the films showed only single broad diffraction in the small angle region at room temperature. Upon heating the films, however, single intense diffraction grew in the small angle region due to the thermal reorganization of the supramolecular structures (Figure 8). These diffractions were accompanied by small diffractions with half and one-third (only for **1**·dCA) of their d -spacing values (Table 2). These XRD patterns indicate that these aggregates form multilamellar structures via the formation of linear tapelike hydrogen bonding motif (Figure 9)^{25,31–34,47} Although no gelation was observed for other systems (**1**·Bar, **2** and **2**·dCA), their thin films prepared from chloroform solutions showed XRD patterns assignable to multilamellar structures upon heating (Supplementary Figure S3 and Table 2).

Proposed hierarchical organization processes of the three gelator systems, **1**, **1**·dCA and **2**·Bar are shown in Figure 9. Despite the fact that two types of mesoscopic structures were clarified for these systems by SEM and AFM, the XRD study indicated that all the aggregates are based on tapelike hydrogen-bonded motif (Figure 9a). In the case of **2**·Bar, PBI moieties can form extended one-dimensional stacks along tapes. For this architecture, supramolecular polymerization (elongation of tapes) might be promoted by π - π stacking in addition to hydrogen bonding interaction (Figure 9b), which results in the formation of one-dimensional nanostructures. In the cases of **1** and **1**·dCA, on the other hand, only dimeric stacks could be formed along tapes due to the dodecyl chains of **1**. Such dimeric units thus can act as interactive sites for the interchain association of the tapes (Figure 9b), which may lead to the formation of two-dimensional sheetlike microstructures.

CONCLUSION

We successfully constructed PBI-based organogel systems by melamine-melamine, melamine-cyanurate and melamine-barbiturate multiple hydrogen bonding interactions. The gelation capability of these systems can be tuned by choosing appropriate solvents, guest molecules and/or the number of chromophore units in melamine molecules. The organogels thus obtained were transparent and showed remarkably low critical gelation concentration of 8.0×10^{-4} M. XRD study revealed that the gelation of solvents was caused by hierarchical organization of tapelike hydrogen-bonded aggregates. However, mesoscopic structures (fibrous and sheetlike

structures) of the aggregates observed by SEM and AFM were different depending on the number of the PBI chromophores in the melamine components. As a result, the gels showed different thermal stabilities. It is proposed that the number of the PBI chromophores introduced in the melamine components can control the hierarchical organization process of the tapelike hydrogen-bonded aggregates. We believe that this modular approach can provide functional soft-materials with well-defined control over the packing structure of functional units and mesoscopic morphologies of the aggregates.

- 1 Schenning, A. P. H. J. & Meijer, E. W. Supramolecular electronics; nanowires from self-assembled π -conjugated systems. *Chem. Commun.* 3245–3258 (2005).
- 2 Rosen, B. M., Wilson, C. J., Wilson, D. A., Peterca, M., Imam, M. R. & Percec, V. Dendron-mediated self-assembly, disassembly, and self-organization of complex systems. *Chem. Rev.* **109**, 6275–6540 (2009).
- 3 Kato, T., Mizoshita, N. & Kishimoto, K. Functional liquid-crystalline assemblies: Self-organized soft materials. *Angew. Chem. Int. Ed.* **45**, 38–68 (2006).
- 4 Würthner, F. Perylene bisimide dyes as versatile building blocks for functional supramolecular architectures. *Chem. Commun.* 1564–1579 (2004).
- 5 Langhals, H. Control of the interactions in multichromophores: Novel concepts. Perylene bis-imides as components for larger functional units. *Helv. Chim. Acta.* **88**, 1309–1343 (2005).
- 6 Yagai, S., Seki, T., Murayama, H., Wakikawa, Y., Ikoma, T., Kikkawa, Y., Karatsu, T., Kitamura, A., Honsho, Y. & Seki, S. Structural and electronic properties of extremely long perylene bisimide nanofibers formed through a stoichiometrically mismatched, hydrogen-bonded complexation. *Small* **6**, 2731–2740 (2010).
- 7 Che, Y., Datar, A., Yang, X., Naddo, T., Zhao, J. & Zang, L. Ultralong nanobelts self-assembled from an asymmetric perylene tetracarboxylic diimide. *J. Am. Chem. Soc.* **129**, 7234–7235 (2007).
- 8 Iverson, I. K. & Tam-Chang, S.-W. Cascade of molecular order by sequential self-organization, induced orientation, and order transfer processes. *J. Am. Chem. Soc.* **121**, 5801–5802 (1999).
- 9 Würthner, F., Thalacker, C., Diele, S. & Tschierske, C. Fluorescent J-Type aggregates and thermotropic columnar mesophases of perylene bisimide dyes. *Chem. Eur. J.* **7**, 2245–2253 (2001).
- 10 Chen, Z., Stepanenko, V., Dehm, V., Prins, P., Siebbeles, L., Seibt, J., Marquetand, P., Engel, V. & Würthner, F. Photoluminescence and conductivity of self-assembled π - π stacks of perylene bisimide dyes. *Chem. Eur. J.* **13**, 436–449 (2007).
- 11 Yagai, S., Monma, Y., Kawauchi, N., Karatsu, T. & Kitamura, A. Supramolecular nanoribbons and nanoropes generated from hydrogen-bonded supramolecular polymers containing perylene bisimide chromophores. *Org. Lett.* **9**, 1137–1140 (2007).
- 12 Seki, T., Yagai, S., Karatsu, T. & Kitamura, A. Miniaturization of nanofibers composed of melamine-appended perylene bisimides and cyanurates. *Chem. Lett.* **37**, 764–765 (2008).
- 13 Sukul, P. K., Asthana, D., Mukhopadhyay, P., Summa, D., Muccioli, L., Zannoni, C., Beljonne, D., Rowan, A. E. & Malik, S. Assemblies of perylene diimide derivatives with melamine into luminescent hydrogels. *Chem. Commun.* **47**, 11858–11860 (2011).
- 14 Sugiyasu, K., Fujita, N. & Shinkai, S. Visible-light-harvesting organogel composed of cholesterol-based perylene derivatives. *Angew. Chem. Int. Ed.* **43**, 1229–1233 (2004).
- 15 Wicklein, A., Ghosh, S., Sommer, M., Würthner, F. & Thelakkat, M. Self-assembly of semiconductor organogelator nanowires for photoinduced charge separation. *ACS Nano* **3**, 1107–1114 (2009).
- 16 Li, X.-Q., Stepanenko, V., Chen, Z., Prins, P., Siebbeles, L. D. A. & Würthner, F. Functional organogels from highly efficient organogelator based on perylene bisimide semiconductor. *Chem. Commun.* 3871–3873 (2006).
- 17 Seki, T., Asano, A., Seki, S., Kikkawa, Y., Murayama, H., Karatsu, T., Kitamura, A. & Yagai, S. Rational construction of perylene bisimide columnar superstructures with biased helical sense. *Chem. Eur. J.* **17**, 3598–3608 (2011).
- 18 Terech, P. & Weiss, R. G. Low molecular mass gelators of organic liquids and the properties of their gels. *Chem. Rev.* **97**, 3133–3159 (1997).
- 19 Ishi-i, T. & Shinkai, S. Dye-based organogels: stimuli-responsive soft materials based on one-dimensional self-assembling aromatic dyes. *Top. Curr. Chem.* **258**, 119–160 (2005).
- 20 Whitesides, G. M., Simanek, E. E., Mathias, J. P., Seto, C. T., Chin, D., Mammen, M. & Gordon, D. M. Noncovalent synthesis: using physical-organic chemistry to make aggregates. *Acc. Chem. Res.* **28**, 37–44 (1995).
- 21 Pronnce, L. J., Reinhoudt, D. N. & Timmerman, P. Noncovalent synthesis using hydrogen bonding. *Angew. Chem. Int. Ed.* **40**, 2382–2426 (2001).
- 22 Yagai, S., Nakajima, T., Kishikawa, K., Kohmoto, S., Karatsu, T. & Kitamura, A. Hierarchical organization of photoresponsive hydrogen-bonded rosettes. *J. Am. Chem. Soc.* **127**, 11134–11139 (2005).
- 23 Yagai, S., Aonuma, H., Kubota, S., Kikkawa, Y., Karatsu, T., Kitamura, A., Mahesh, S. & Ajayaghosh, A. Rational design of nanofibers and nanorings through complementary hydrogen-bonding interactions of functional π systems. *Chem. Eur. J.* **16**, 8652–8661 (2010).

- 24 Yagai, S., Nakano, Y., Seki, S., Asano, A., Okubo, T., Isoshima, T., Karatsu, T., Kitamura, A. & Kikkawa, Y. Supramolecularly engineered aggregation of a dipolar dye: Vesicular and ribbonlike architectures. *Angew. Chem. Int. Ed.* **49**, 9990–9994 (2010).
- 25 Seki, T., Yagai, S., Karatsu, T. & Kitamura, A. Formation of Supramolecular polymers and discrete dimers of perylene bisimide dyes based on melamine-cyanurates hydrogen-bonding interactions. *J. Org. Chem.* **73**, 3328–3335 (2008).
- 26 Seki, T., Maruya, Y., Nakayama, K., Karatsu, T., Kitamura, A. & Yagai, S. Solution processable hydrogen-bonded perylene bisimide assemblies organizing into lamellar architectures. *Chem. Commun.* **47**, 12447–12449 (2011).
- 27 Yagai, S., Kinoshita, T., Higashi, M., Kishikawa, K., Nakanishi, T., Karatsu, T. & Kitamura, A. Diversification of self-organized architectures in supramolecular dye assemblies functional dyes are essential for miniaturizing optoelectronic. *J. Am. Chem. Soc.* **129**, 13277–13287 (2007).
- 28 Yagai, S. Supramolecular complexes of functional chromophores based on multiple hydrogen-bonding interactions. *J. Photochem. Photobiol. C* **7**, 164–182 (2006).
- 29 Langhals, H., Demmig, S. & Potrawa, T. The relation between packing effects and solid state fluorescence of dyes. *J. Prakt. Chem.* **333**, 733–748 (1991).
- 30 Wickelein, A., Lang, A., Muth, M. & Thelakkat, M. Swallow-tail substituted liquid crystalline perylene bisimides: synthesis and thermotropic properties. *J. Am. Chem. Soc.* **131**, 14442–14453 (2009).
- 31 Hanabusa, K., Miki, T., Taguchi, Y., Koyama, T. & Shirai, H. J. Two-component, small molecule gelling agents. *J. Chem. Soc. Chem. Commun.* 1382–1384 (1993).
- 32 Koyano, H., Bissel, P., Yoshihara, K., Ariga, K. & Kunitake, T. Syntheses and interfacial hydrogen-bonded network of hexaalkyl Tris(Melamine) amphiphiles. *Langmuir* **13**, 5426–5432 (1997).
- 33 Kimizuka, N., Kawasaki, T., Hirata, K. & Kunitake, T. Supramolecular membranes. spontaneous assembly of aqueous bilayer membrane via formation of hydrogen bonded pairs of melamine and cyanuric acid derivatives. *J. Am. Chem. Soc.* **120**, 4094–4104 (1998).
- 34 Würthner, F., Yao, S., Heise, B. & Tschierske, C. Hydrogen bond directed formation of liquid-crystalline merocyanine dye assemblies. *Chem. Commun.* 2260–2261 (2001).
- 35 Yagai, S., Seki, T., Karatsu, T., Kitamura, A. & Würthner, F. Transformation from H- to J-Aggregated perylene bisimide dyes by complexation with cyanurates. *Angew. Chem. Int. Ed.* **47**, 3367–3371 (2008).
- 36 *Low Molecular Mass Gelators (Topics in Current Chemistry)* (ed. Fages, F.) Vol 256 (Springer, Berlin (Germany), 2005).
- 37 Zerkowski, J. A., Seto, C. T. & Whitesides, G. M. Solid-state structures of rosette and crinkled tape motifs derived from the cyanuric acid melamine lattice. *J. Am. Chem. Soc.* **114**, 5473–5475 (1992).
- 38 Mathias, J. P., Simanek, E. E., Zerkowski, J. A., Seto, C. T. & Whitesides, G. M. Structural preferences of hydrogen-bonded networks in organic solution—the cyclic CA₃·M₃ 'Rosette'. *J. Am. Chem. Soc.* **116**, 4316–4325 (1994).
- 39 Bielejewska, A. G., Marjo, C. E., Prins, L. J., Timmerman, P., de Jong, F. & Reinhoudt, D. N. Thermodynamic stabilities of linear and crinkled tapes and cyclic rosettes in melamine-cyanurate assemblies: A model description. *J. Am. Chem. Soc.* **123**, 7518–7533 (2001).
- 40 Würthner, F., Thalacker, C., Sautter, A., Schärtl, W., Ibach, W. & Hollricher, O. Hierarchical self-organization of perylene bisimide-melamine assemblies to fluorescent mesoscopic superstructures. *Chem. Eur. J.* **6**, 3871–3885 (2000).
- 41 Ghiviriga, I. & Oniciu, D. C. Steric hindrance to the solvation of melamines and consequences for non-covalent synthesis. *Chem. Commun.* 2718–2719 (2002).
- 42 Bouas-Laurent, H. & Desvergne, J.-P. *Molecular Gels: Materials with Self-Assembled Fibrillar Networks* (ed. Weiss, R. G. & Terech, P.) ch. 12 (Springer, Netherlands, 2006).
- 43 Zubarev, E. R., Pralle, M. U., Sone, E. D. & Stupp, S. I. Scaffolding of polymers by supramolecular nanoribbons. *Adv. Mater.* **14**, 198–203 (2002). See also reference [14].
- 44 Jung, J. H., Ono, Y. & Shinkai, S. Novel silica structures which are prepared by transcription of various superstructures formed in organogels. *Langmuir* **16**, 1643–1649 (2000).
- 45 Yagai, S., Iwashima, T., Kishikawa, K., Nakahara, S., Karatsu, T. & Kitamura, A. Photoresponsive self-assembly and self-organization of hydrogen-bonded supramolecular tapes. *Chem. Eur. J.* **12**, 3984–3994 (2006).
- 46 Watanabe, Y., Miyasou, T. & Hayashi, M. Diastereomixture and racemate of myo-inositol derivatives, stronger organogelators than the corresponding homochiral isomers. *Org. Lett.* **6**, 1547–1550 (2004).
- 47 Thalacker, C. & Würthner, F. Chiral perylene bisimide–melamine assemblies: hydrogen bond-directed growth of helically stacked dyes with chiroptical properties. *Adv. Funct. Mater.* **12**, 209–218 (2002).

Supplementary Information accompanies the paper on Polymer Journal website (<http://www.nature.com/pj>)